THE JOURNAL OF BIOLOGICAL CHEMISTRY VOL. 287, NO. 21, pp. 17870–17881, May 18, 2012

Two Chimeric Regulators of G-protein Signaling (RGS) Proteins Differentially Modulate Soybean Heterotrimeric G-protein Cycle*[S]

Received for publication, February 14, 2012, and in revised form, March 26, 2012 Published, JBC Papers in Press, April 2, 2012, DOI 10.1074/jbc.M112.353219

Swarup Roy Choudhury[‡], Corey S. Westfall[§1], John P. Laborde[‡2], Naveen C. Bisht[‡3], Joseph M. Jez[§], and Sona Pandey[‡4]

From the [‡]Donald Danforth Plant Science Center, St. Louis, Missouri 63132 and the [§]Department of Biology, Washington University, St. Louis, Missouri 63130

Background: The soybean genome encodes the most expanded plant heterotrimeric G-protein network reported to date.
Results: Each Gα has distinct biochemical properties, and the RGS proteins have different GTPase-activating effects on each Gα.
Conclusion: The core G-protein components, their interactions, and biochemical properties are conserved across phyla, but important mechanistic differences exist.
Significance: This study provides insight into the complexity of plant G-protein networks.

Heterotrimeric G-proteins and the regulator of G-protein signaling (RGS) proteins, which accelerate the inherent GTPase activity of Gα proteins, are common in animals and encoded by large gene families; however, in plants G-protein signaling is thought to be more limited in scope. For example, *Arabidopsis thaliana* contains one Gα, one Gβ, three Gγ, and one RGS protein. Recent examination of the *Glycine max* (soybean) genome reveals a larger set of G-protein-related genes and raises the possibility of more intricate G-protein networks than previously observed in plants. Stopped-flow analysis of GTP-binding and GDP/GTP exchange for the four soybean Gα proteins (GmGα1–4) reveals differences in their kinetic properties. The soybean genome encodes two chimeric RGS proteins with an N-terminal seven transmembrane domain and a C-terminal RGS box. Both GmRGS interact with each of the four GmGα and regulate their GTPase activity. The GTPase-accelerating activities of GmRGS1 and -2 differ for each GmGα, suggesting more than one possible rate of the G-protein cycle initiated by each of the Gα proteins. The differential effects of GmRGS1 and GmRGS2 on GmGα1–4 result from a single valine *versus* alanine difference. The emerging picture suggests complex regulation of the G-protein cycle in soybean and in other plants with expanded G-protein networks.

Heterotrimeric G-proteins are important signal transducers in all eukaryotes. Signal transduction by G-proteins depends on the guanine nucleotide-bound status of the Gα protein that switches between GDP·Gα and GTP·Gα to represent "off" and "on" signaling modes, respectively (1, 2). This classic system entails three biochemically distinct steps that control all physiological responses regulated by G-proteins: the rate of GTP binding, the rate of GTP hydrolysis, and the rate of GDP/GTP exchange. The biochemical properties of the G-protein cycle necessitate precise regulation of each step. In mammalian systems, networks of regulatory proteins provides exquisite control of the G-protein cycle (3). The human genome, for example, encodes over 1,000 G-protein-coupled receptors (GPCR).[5] The GPCR act as specific guanine nucleotide exchange factors for different Gα proteins to promote GDP/GTP exchange (4), which is the rate-limiting step of the G-protein signaling cycle (5, 6). The rate of GTP hydrolysis in Gα proteins is enhanced by regulator of G-protein signaling (RGS) proteins (3, 4, 7), which act as GTPase-activating proteins (GAPs) to promote continuous G-protein cycling, thereby accelerating both signal onset and decay.

In plants, understanding the heterotrimeric G-protein signaling mechanisms is still in its infancy, with most data coming from *Arabidopsis* and rice. Both of these plants possess a limited repertoire of heterotrimeric G-proteins with one Gα, one Gβ, and three Gγ subunits, whereas the human genome encodes for 23 Gα, 5 Gβ, and 12 Gγ subunits (8–10). Likewise, there is a single RGS protein in *Arabidopsis* but 37 in humans (8, 11). The rice genome does not encode any obvious candidate for an RGS protein (9, 12). Despite their limited quantities, plant G-proteins are involved in multiple signaling pathways

* This work was supported in part by United States Department of Agriculture/Agriculture and Food Research Initiative Grant 2010-65116-20454 (to S. P.).
[S] This article contains supplemental Figs. S1–S3 and Tables S1 and S2.
[1] Supported by United States Department of Agriculture/Agriculture and Food Research Initiative Pre-doctoral Research Fellowship MOW-2010-05240.
[2] Supported by National Science Foundation Research Experiences for Undergraduates Grant NSF-MCB-0851838. Present address: Liberty University, Lynchburg, VA 24502.
[3] Supported by a visiting scholar fellowship from the National Institute of Plant Genome Research, New Delhi, India. Present address: National Institute of Plant Genome Research, New Delhi, India 110067.
[4] To whom correspondence should be addressed: Donald Danforth Plant Science Center, 975 North Warson Rd., St. Louis, MO 63132. Tel.: 314-587-1471; Fax: 314-587-1571; E-mail: spandey@danforthcenter.org.

[5] The abbreviations used are: GPCR, G-protein-coupled receptor; BODIPY, 4,4-difluoro-4-bora-3α,4α-diazaindacene; GAP, GTPase-activity accelerating protein; MANT, 2′-/3′-*O*-*N*′-methylanthraniloyl; RGS, regulator of G-protein signaling; CUb, C-terminal half of ubiquitin; NUb, N-terminal half of ubiquitin; EYFP, enhanced YFP; 7-TM, 7-transmembrane.

controlling various aspects of growth and development (12–21).

We have recently identified an elaborate G-protein family in soybean that has greatly expanded the diversity and complexity of plant G-protein networks. The soybean genome encodes four Gα, four Gβ, and ten Gγ subunits, suggesting more than a hundred possible heterotrimeric combinations compared with three in *Arabidopsis* (10, 22, 23). Moreover, the expression patterns and interaction specificity of G-protein subunits suggest the formation of tissue- and signal-specific heterotrimers in soybean, as reported in mammals (24–27).

Detailed biochemical characterization of the different steps of G-protein cycling in plants is currently limited to the *Arabidopsis* Gα protein AtGPA1 and its regulatory RGS protein AtRGS1 (11, 28–30). AtGPA1 is an extremely slow GTPase with significantly high rates of GTP binding and GDP release and is proposed to exist almost entirely in the GTP-bound conformation. Based on these observations, GTP hydrolysis by AtGPA1 is proposed as the rate-limiting step of the *Arabidopsis* G-protein signaling cycle (28, 31), in contrast to the GDP/GTP exchange of Gα proteins in mammalian G-protein signaling (2, 4).

Initial biochemical analysis of GmGα1–4 predicted important kinetic differences among them. For example, group II GmGα proteins (GmGα2 and GmGα3) exhibited a faster rate of GTP -hydrolysis than group I GmGα proteins (GmGα1 and GmGα4) and AtGPA1 (23). This study was designed to compare the GTP-binding rates and GDP/GTP exchange rates of GmGα1–4 and to examine the role of two soybean RGS proteins (GmRGS1 and GmRGS2) on the intrinsic GTPase activity of the GmGα proteins. Our data show that each GmGα protein has a distinct rate of GTP binding and GTPase activity. The two GmRGS proteins exert differential GAP activities on each of the GmGα proteins, and the difference in their GAP activity results from a single valine *versus* alanine alteration. These results suggest a complex regulation of the G-protein cycle in soybean and, by extension, in other plants with expanded G-protein networks.

EXPERIMENTAL PROCEDURES

Plant Material and Growth Conditions—Soybean (*Glycine max* L.) cv. Jack seeds were grown in a growth chamber (26/20 °C day/night temperature, photoperiod of 14/10 h, 800 μmol m^{-2} s^{-1} light intensity, and 60% humidity). Tissue samples for different stages were prepared as described previously (23).

Cloning of Soybean RGS Protein Genes and Recombinant Protein Purification—Soybean RGS protein genes were identified by BLAST analysis of the latest *G. max* genome assembly using *Arabidopsis* and mammalian RGS protein sequences as queries. Full-length *GmRGS* genes were amplified from soybean seedling cDNA using gene-specific primers (supplemental Table S1), cloned into the pENTR/D-TOPO vector (Invitrogen), and confirmed by sequencing. The RGS domains of GmRGS1 and GmRGS2 (amino acids 251–464) were cloned into pET-28a (Novagen, WI) and transformed into *E. coli* Rosetta cells (Novagen). Recombinant proteins were purified using Ni^{2+}-affinity chromatography (32). Protein aliquots were snap-frozen in liquid nitrogen and stored at −80 °C. Mutant GmRGS constructs were prepared by site-directed mutagenesis using the QuikChange PCR method (Agilent). Protein expression and purification were as for the wild-type GmRGS. The four GmGα proteins were purified as described previously (23).

RNA Isolation and Quantitative RT-PCR—RNA isolation and quantitative real time PCR were performed as described previously (23). The oligonucleotides used for PCR are listed in supplemental Table S1. Experiments were repeated three times, and data were averaged.

Protein-Protein Interaction Assays—The interaction assay between GmGα and GmRGS was performed using the mating-based yeast split-ubiquitin system (33). Briefly, full-length *GmRGS1–2* genes were fused with the C-terminal half of ubiquitin (CUb fusions) and the *GmGα1–4* genes were fused with the N-terminal half of ubiquitin (NUb fusions). NUb fusions with each *GmGα* were created in both N- and C-terminal orientations (*i.e.* GmGα-NUb and NUb-GmGα). NUb_{wt} fusion constructs, which exhibit intrinsic interaction with CUb fusion constructs, were used as positive controls. Yeast transformations and mating were performed as in Bisht *et al.* (23). For the split-ubiquitin interaction assays, yeast were grown on minimal media lacking leucine, tryptophan, histidine, and adenine, in the presence of 1 mM methionine. For *in planta* interactions, the *GmGα1–4* genes were cloned into 77 nEYFP-N1 vectors (containing nEYFP at the C-terminal end; see Ref. 34), and the *GmRGS1–2* genes were cloned into 78 cEYFP-N1 vectors (containing cEYFP at the C-terminal end; Ref. 34). All constructs were transformed into *Agrobacterium tumefaciens* strain GV3101, resuspended in AS medium (10 mM $MgCl_2$, 150 μM acetosyringone and 10 mM MES, pH 5.7) to A_{600} = 0.8, and co-infiltrated in the abaxial side of tobacco leaves. The leaves were imaged 36 h post-infiltration with the Nikon Eclipse E800 microscope with epi-fluorescence module for YFP fluorescence detection. At least four independent transformations were performed for each construct. Localization of *GmRGS-YFP* was performed as described previously (22).

G-protein and RGS Protein Activity Assay—The kinetics of GTP-binding and GTP/GDP exchange were determined by stopped-flow analysis using an Olis DM45 spectrofluorimeter with a 150-watt xenon lamp and stopped-flow accessory. Fluorescence resonance energy transfer (FRET) signal between tryptophan and the 2′-/3′-*O*-*N*′-methylanthraniloyl) (MANT) group (from either MANT-GTP or MANT-GDP, λ_{ex} = 280 nm with a cutoff filter >420 nm) was followed to measure the rate of GTP-binding exchange and GDP/GTP exchange. Assays were performed at 20 °C in 20 mM Tris, pH 8.0, 100 mM NaCl, and 10 mM $MgCl_2$. An average of 8–11 scans were collected for each condition and normalized. KintekGlobal Kinetic Explorer version 2.5 (35) was used to fit the binding data using a model describing binding followed by a conformational change. Exchange of MANT-GDP with GTP was fit to a single exponential curve.

Real time fluorescence-based GTP binding and GTP hydrolysis assays were performed using BODIPY-GTP FL (36). Assays were performed at 25 °C in a 200-μl reaction volume of assay buffer (20 mM Tris, pH 8.0, and 10 mM $MgCl_2$). The reaction was started by addition of labeled nucleotide. For each assay, 250 nM of GmGα protein was used. To evaluate the GAP activ-

ity of each GmRGS, 500 nM of protein was incubated with GmGα, and fluorescence (λ_{ex} = 485 nm, λ_{em} = 530 nm) was recorded every 16 s for up to 54 min using a fluorescence microplate reader (FLUOstar Optima, BMG Lab Technologies).

GAP activity of GmRGS1 and GmRGS2 was also assayed using the ENZchek phosphate assay kit (Invitrogen). Each GmGα (5 μM) was pre-loaded with GTP (1 mM) and incubated with 0.1–2 μM of GmRGS. Phosphate (P_i) production was recorded as a change in absorbance at 360 nm using a Spectramax M2 spectrophotometer (Molecular Devices, Sunnyvale, CA) for up to 30 min at 25 °C. The amount of P_i released was evaluated from the corresponding values obtained with a standard curve. Data were plotted as nanomoles of P_i released min^{-1} mg^{-1} of GmRGS and fit using nonlinear regression in GraphPad Prism version 5.0.

RESULTS

Analysis of GTP Binding and GTP/GDP Exchange in GmGα1–4—Initial BODIPY-fluorescence assays suggested that GmGα1–4 may have different GTP binding, hydrolysis, and/or exchange kinetics (23). To further examine the properties of each GmGα, the rate of GTP binding and GDP release were determined using MANT-GTP and MANT-GDP analogs, respectively, in a stopped-flow assay system.

For GTP binding, 1 μM of each GmGα protein was examined with varied concentrations of MANT-GTP (Fig. 1*A*). The rate constants (k_{on}) derived from the data (Table 1) indicate that GmGα1 and GmGα4 bind GTP more rapidly than GmGα2 and GmGα3. In addition, the GTP-binding rates of all four GmGα proteins are faster than AtGPA1 (k_{on} = 1.1 ± 0.1), which is also 2 orders of magnitude faster than mammalian G-proteins (28).

To assess the rate of GDP release from GmGα, 1 μM of each of the proteins was preincubated with 5 μM MANT-GDP. An excess (160 μM) of unlabeled GTP was then used to start the reaction, and the GTP/GDP exchange rate was determined. Fig. 1*B* shows the kinetics of MANT-GDP/GTP exchange for GmGα3 and GmGα4. GmGα3 exhibits a lower rate of GDP/GTP exchange compared with GmGα4. The reactions for GmGα1 and GmGα2 essentially overlap with that of GmGα4 and are not shown for the sake of clarity. Table 1 summarizes the comparative rates of MANT-GTP binding and MANT-GDP/GTP exchange for GmGα1–4.

For GmGα1–4, the GTP hydrolysis rate of each protein in the absence of an RGS protein was very slow, and only approximate values derived from the single turnover reactions were determined (supplemental Table S2). The k_{cat} value for GmGα2 was 0.055 min^{-1}, which was similar to the rate of AtGPA1 GTPase activity (0.063 min^{-1}) reported previously (28, 31). This extremely slow rate of GTP hydrolysis of GmGα proteins together with the rate of nonenzymatic GTP hydrolysis made it difficult to compare the small quantitative differences between GmGα proteins and to evaluate K_m values.

Soybean Genome Encodes Two Chimeric Proteins with RGS Domains—In most organisms, the expansion and diversity of Gα proteins correlate with the expansion and diversity of RGS proteins (37). The only exception known to date is rice, which contains a Gα protein and lacks an RGS protein (12). To determine whether RGS proteins are as prevalent in plants as they are in animals, and whether genome duplication led to an expansion of RGS proteins in soybean similar to that reported for the Gα proteins (23), we queried the soybean data base using *Arabidopsis* and animal RGS protein sequences.

Genome analysis identified one or more homologs of AtRGS1 in all dicot plants but none in monocot plants (with the

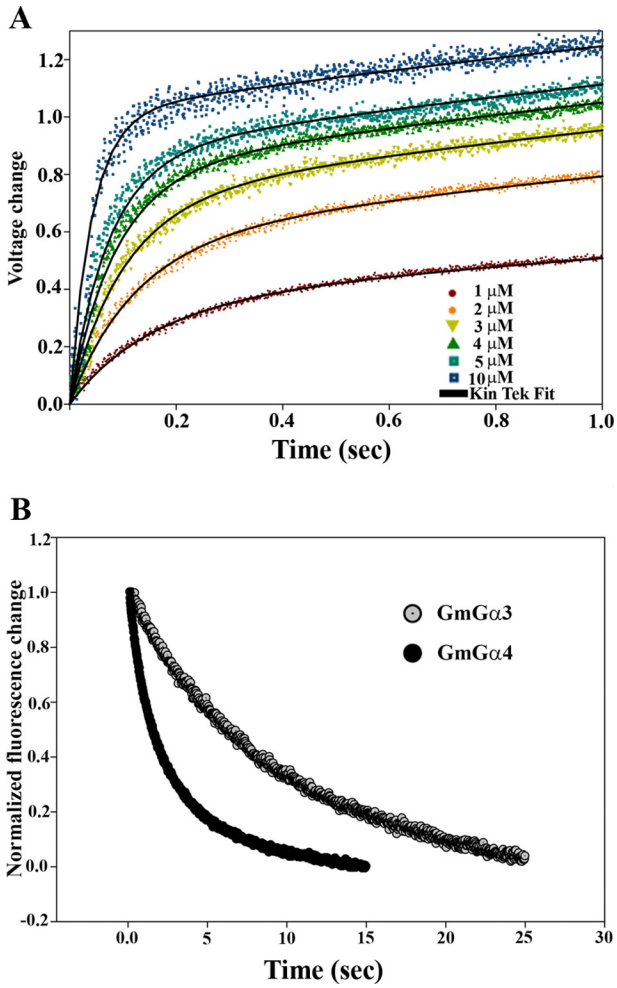

FIGURE 1. **GmGα have distinct rates of GTP binding and GDP/GTP exchange.** *A,* kinetics of GTP binding of GmGα3. GmGα3 (1 μM) was incubated with 1–10 μM of MANT-GTP, and FRET signal between tryptophan (λ_{ex} = 280 nm) was measured using an Olis DM45 spectrofluorimeter with stopped-flow accessory. Similar data were obtained for other GmGα (not shown). Data were fit using KintekGlobal Kinetic Explorer using a model for binding followed by a conformational change. *B,* comparison of GDP/GTP exchange kinetics of GmGα3 and GmGα4. GmGα (1 μM) was pre-loaded with 5 μM MANT-GDP. Unlabeled GTP (160 μM) was then shot into the reaction, and the rate of GTP/GDP exchange was followed by measuring the change in fluorescence due to FRET signal between tryptophan and MANT *versus* time. Curves for GmGα1 and GmGα2 overlapped with GmGα4 and are not shown for clarity. Exchange of MANT-GDP with GTP was fit to a single exponential curve.

TABLE 1
Comparative kinetics of GmGα proteins
All values are expressed as a mean ± S.E. (n = 3).

Proteins	MANT-GTP binding k_{on}	MANT-GDP dissociation k_{off}
	μM^{-1} min^{-1}	min^{-1}
GmGα1	4.0 ± 0.1	41.0 ± 0.5
GmGα2	2.8 ± 0.4	28.9 ± 0.4
GmGα3	2.2 ± 0.1	8.6 ± 0.1
GmGα4	8.0 ± 2.3	32.9 ± 0.2

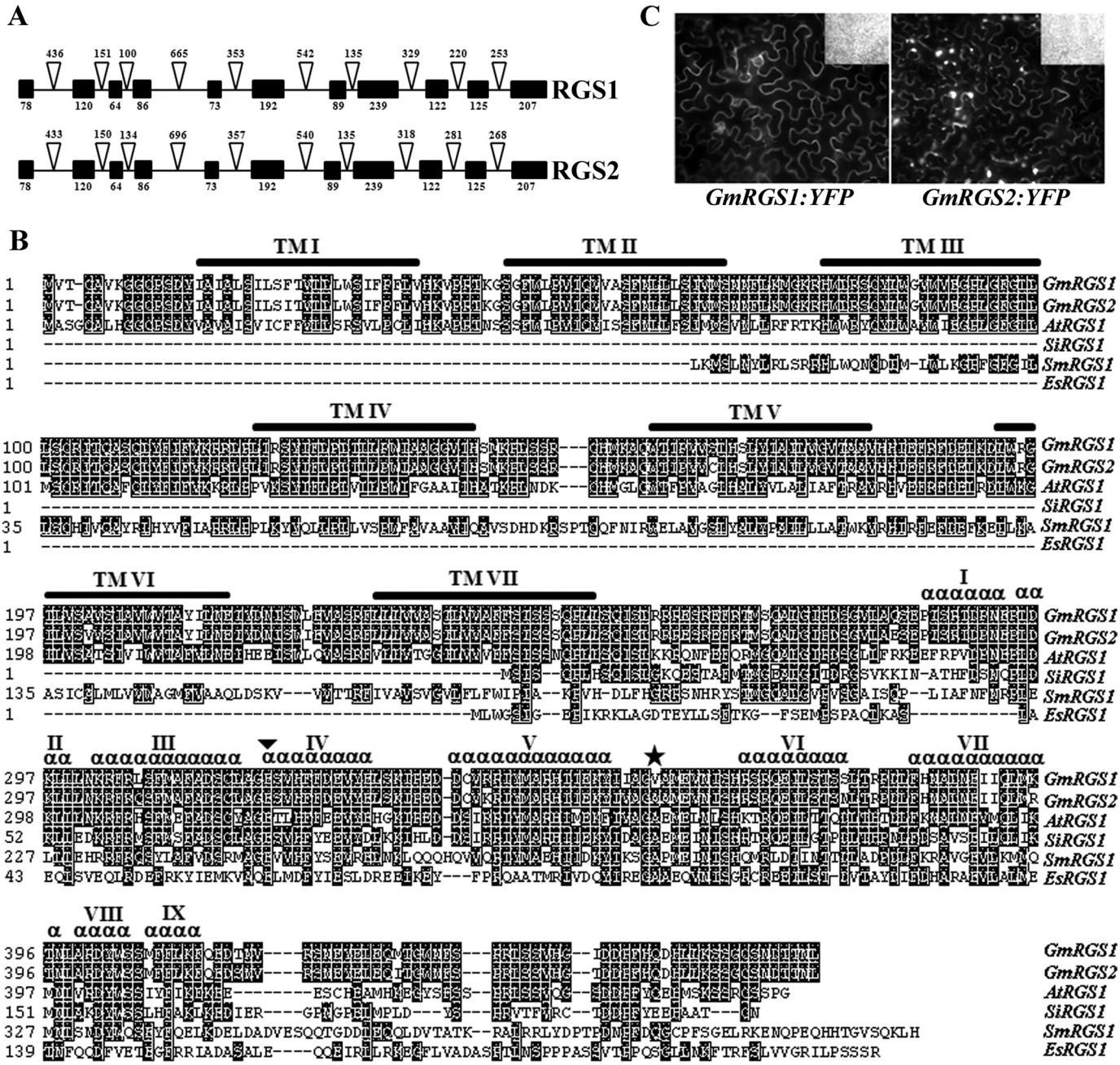

FIGURE 2. **Sequence features and localization of GmRGS proteins.** *A,* exon/intron organization of *GmRGS* genes. *Black boxes* represent exons and *triangles* represent introns. The *numbers* at the *bottom* and *top* represent exon and intron lengths, respectively. *B,* most plant RGS proteins are chimeric proteins with N-terminal 7TM domain and C-terminal RGS domain. Amino acid sequence alignment of *Arabidopsis*, soybean, *S. italica*, *Selaginella moellendorffii,* and *Ectocarpus siliculosus* RGS proteins was performed using Clustal W. The position of the seven transmembrane domains was determined by TMHMM server, version 2.0. The predicted domains are marked with *horizontal lines* on the *top* and are numbered *TM I* to *TM VII*. The nine α-helices of the RGS domains are represented and marked with *I* to *IX*. ▼ represents the conserved Glu-319 crucial for RGS protein activity and binding with Gα proteins, and the *star* represents amino acid identified in this study as responsible for slow activity of GmRGS1. The amino acid positions are numbered in accordance with GmRGS1. *C, YFP-GmRGS* is localized to the cell periphery in transiently transformed tobacco leaves. At least three independent transformations were performed. The figure shows representative picture from each transformation.

exception of *Setaria italica*, see supplemental Fig. S1). The soybean genome has two loci (Glyma18g01490.1 and Glyma11g37540.1) with 64% sequence identity to AtRGS1 (11). These are renamed *GmRGS1* and *GmRGS2*, respectively. The *GmRGS1* gene is mis-annotated in the current version of the soybean genome with a predicted protein lacking the first exon as identified here. Discrepancies between the reported and experimentally validated sequence of the *GmRGS2* gene were also identified. The correct sequences of both these genes and their exon-intron boundaries are detailed in supplemental Figs. S2 and S3.

GmRGS1 and *GmRGS2* each encode open reading frames of 464 amino acids that share 96% identity, which suggests their origin from a recent genome duplication event (38). This was corroborated by the analysis of their chromosomal location and exon-intron architecture. Both genes contain 11 exons and 10

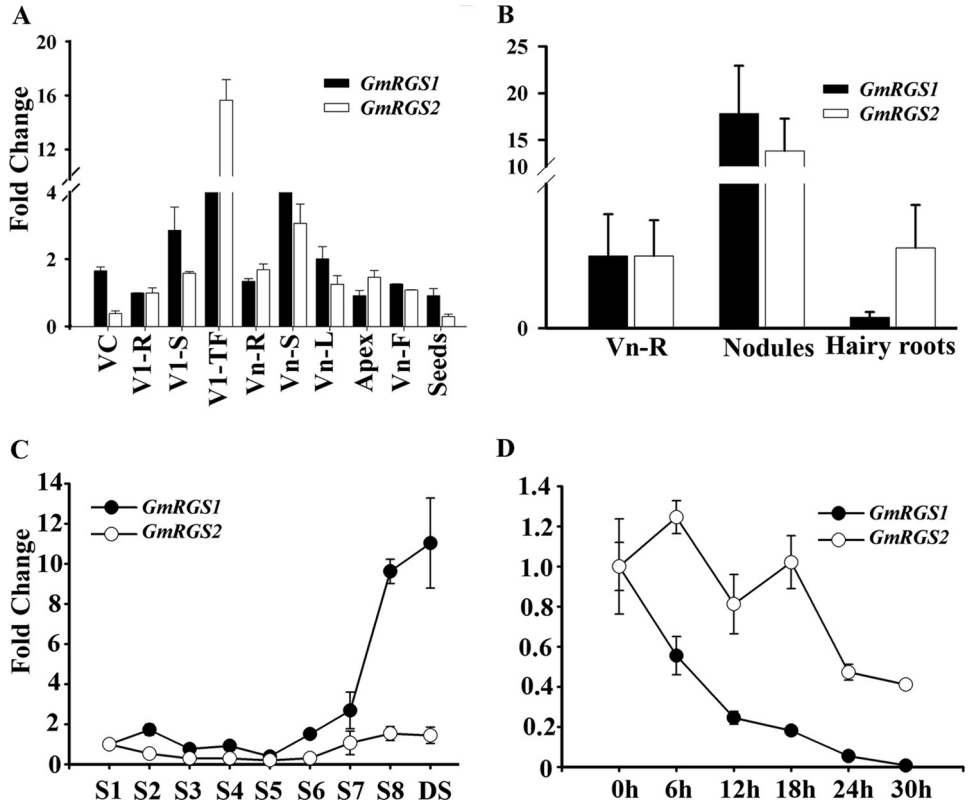

FIGURE 3. ***GmRGS* genes have distinct expression patterns.** *A,* expression of *GmRGS* genes in different tissue types. The stages are defined as follows: *VC*, cotyledon; *V1-R*, primary root at stage V1 (appearance of the first set of unfolded trifoliolate leaves); *V1-S*, primary stem at stage V1; *V1-TF*, first trifoliate leaf; *Vn-R*, mature root; *Vn-S*, mature stem; *Vn-L*, mature leaves; *Apex*, shoot apex; *Vn-F*, flower; *S4*, seed stage S4. Expression in V1-R roots was set at 1. *B,* expression of *GmRGS* genes in nodules and hairy roots. Expression in mature roots (Vn-R) is set at 1. *C,* expression of *GmRGS* genes during different stages of seed development. The seed development stages (*S1–S8*) are according to Ref. 41. Dry seed (*DS*) stage was also used for the analysis. The expression in seeds at S1 was set at 1. *D,* expression of *GmRGS* genes during seed germination. Seed germination was followed starting from dry seeds (0 h) up to 30 h when an obvious radical had protruded. Seed samples were collected at every 6 h following imbibition of dry seeds. The expression in dry seeds at 0 h was set at 1. For each data set quantitative RT-PCR amplification experiments were performed three times independently for each target, and the data were averaged. The expression values were normalized against soybean *Actin* gene expression. *Error bars* represent the mean ± S.E.

introns with highly conserved exon lengths (Fig. 2*A*) and are present on the duplicated regions of the chromosomes.

The GmRGS proteins share both common sequence features and cellular localization with AtRGS1. Both GmRGS proteins display a chimeric architecture with an N-terminal 7-transmembrane (7TM) domain (amino acids 15–252), as found in classic GPCRs, and a C-terminal RGS box (amino acids 294–412) (Fig. 2*B*). The RGS box of each GmRGS contains nine predicted α-helical regions typical of all RGS proteins (Fig. 2*B*). The predicted secondary structure of each GmRGS C-terminal domain aligns with mammalian homologs as determined by I-TASSER (39). None of the mammalian RGS box-containing proteins have a 7TM GPCR-like domain associated with them, although such domains have been identified in some protozoan and many fungal RGS proteins (37). Intriguingly, the sole representative of a monocot plant RGS protein from *S. italica* lacks the N-terminal 7TM domain (Fig. 2*B*). Both GmRGS proteins also contain two cysteine residues (*i.e.* Cys-83 and Cys-153) that may form a disulfide linkage found in many GPCRs (11). In addition, both GmRGS localized to the cell periphery (Fig. 2*C*), which is similar to the localization of AtRGS1 (11).

GmRGS Proteins Have Overlapping Expression Patterns with Gα Proteins—Previous work reported the expression patterns of *GmGα1–4* in different tissues of soybean and at various growth and development phases (23). Because RGS proteins work with Gα proteins to regulate G-protein signaling, the degree of overlap between the expression of specific *GmGα* and *GmRGS* genes was evaluated using real time quantitative PCR.

Similar to the expression of *GmGα* genes, the two *GmRGS* genes are expressed widely in most organs and tissue types (Fig. 3*A*). Moreover, both *GmRGS* genes were expressed at a very high level in the first trifoliate leaf, which is similar to the expression pattern of *GmGα4* (23).

The role of the G-protein during nodulation has been analyzed in legumes (40), and two of the soybean *Gα* genes (*i.e. GmGα1* and *GmGα3*) are expressed at a very high level in nodules compared with non-nodulating roots (23). Our results show that both *GmRGS* genes have 12–15-fold higher expression in nodules compared with non-nodulating mature roots (Fig. 3*B*). The expression analysis suggests potential isoform-specific roles for GmGα1 and GmGα3 in nodulation.

The four *GmGα* genes also exhibited interesting expression profiles during seed development and seed germination (23). Given the role of G-proteins during seed germination in *Arabidopsis* and rice and the importance of soybean seeds as food and feed, we compared the expression patterns of the two *GmRGS* genes during seed development and germination. During seed development (defined here as stages S1–S8; see Ref. 41), the

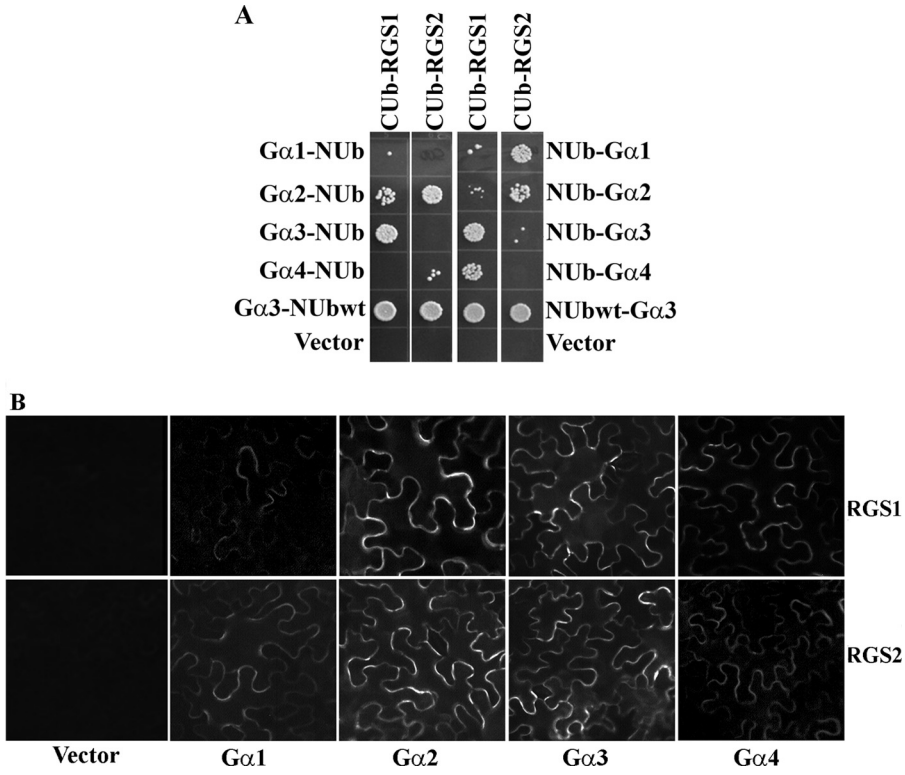

FIGURE 4. **GmRGS proteins interact with GmGα proteins.** *A,* interaction between GmRGS and GmGα proteins using split ubiquitin-based interaction assay. The picture shows yeast growth on selective media with 1 mM methionine. In all cases, GmGα proteins were used as NUb fusions in both orientations (NUb-GmGα denoting NUb fused to the N terminus of GmGα and GmGα-NUb denoting NUb fused to the C terminus of GmGα) and RGS proteins as CUb fusions. NUb_{wt} fusion constructs were used as positive controls for interaction, and NUb vectors were used as negative controls. Two biological replicates of the experiment were performed with identical results. *B,* interaction between GmRGS (in 77-nEYFP-N1) and GmGα (in 78-cEYFP-N1) proteins using bimolecular complementation assay. Agrobacteria containing different combinations of GmRGS and GmGα were infiltrated in tobacco leaves, and reconstitution of YFP fluorescence due to protein-protein interaction was visualized with a microscope (34). At least four independent infiltrations were performed for each protein combination with similar results.

GmRGS1 transcript level remained relatively constant through S7, followed by a greater than 10-fold increase at S8 and in dry seeds (Fig. 3*C*). Conversely, expression of *GmRGS2* during seed development did not change. The expression profile of *GmRGS1* correlates with that of the group II *GmGα* (*Gα2* and *Gα3*), whereas *GmRGS2* expression corresponds to expression of the group I *GmGα* (*Gα1* and *Gα4*).

Expression of *GmRGS1* and *GmRGS*2 genes was also analyzed during soybean seed germination. Previous work showed that all four *GmGα* genes are expressed at significantly higher levels up to 12 h post-imbibition, followed by a gradual decrease (23). The expression of *GmRGS1* and *GmRGS2* genes, however, showed an overall decrease following imbibition (Fig. 3*D*).

GmRGS Proteins Interact with GmGα Proteins—Computer modeling studies suggest that amino acids crucial for RGS1 and Gα interaction are conserved between mammalian and plant homologs (28). AtGPA1 interacts with full-length AtRGS1, as well as the RGS domain of the same protein (11, 28). In non-plant systems, where multiple Gα and RGS proteins exist in a single organism, a high degree of interaction specificity occurs between particular Gα and RGS proteins (42, 43).

To assess interaction between GmGα and GmRGS proteins, the eight possible interaction combinations (four GmGα × two RGS proteins) were tested using the membrane-based split ubiquitin system (33). For this experiment, GmRGS1 and GmRGS2 were used as bait proteins (CUb fusions) and GmGα1–4 as prey proteins (NUb fusions). NUb fusions with GmGα proteins were made in both orientations, NUb-GmGα and GmGα-NUb, resulting in 16 different test interactions. Each GmRGS interacts with all four GmGα proteins, in at least one orientation (Fig. 4*A*). To confirm the yeast-based interaction data, bimolecular fluorescence complementation was used *in planta* to test for interaction between the two protein combinations (34). Each *GmGα* was cloned as an N-terminal fusion to the C terminus of YFP (*Gα-cYFP*). Each *GmRGS* was cloned as an N-terminal fusion to the N terminus of YFP (*RGS-nYFP*). Interactions were examined by co-infiltrating specific RGS and Gα combinations and looking for reconstitution of YFP fluorescence in the infiltrated tobacco leaves. YFP fluorescence was observed in all eight possible combinations confirming that both GmRGS can interact with each GmGα *in vivo* (Fig. 4*B*).

RGS Proteins Act as GAPs for the GmGα—To establish that GmRGS interact with GmGα and function as GAPs, we assayed their effect on the GTPase activity of GmGα1–4. Full-length cDNAs corresponding to *GmGα1–4* and the RGS domain of *GmRGS1–2* (amino acids 251–464) were expressed as recombinant proteins in *E. coli* and purified by Ni^{2+}-affinity chromatography. Each protein was purified to greater than 95% purity (Fig. 5*A*).

Fluorescence-based real time assays were performed to evaluate the effect of each GmRGS on the GTPase activity of each GmGα using BODIPY-GTP. In this assay, the slope of the curve

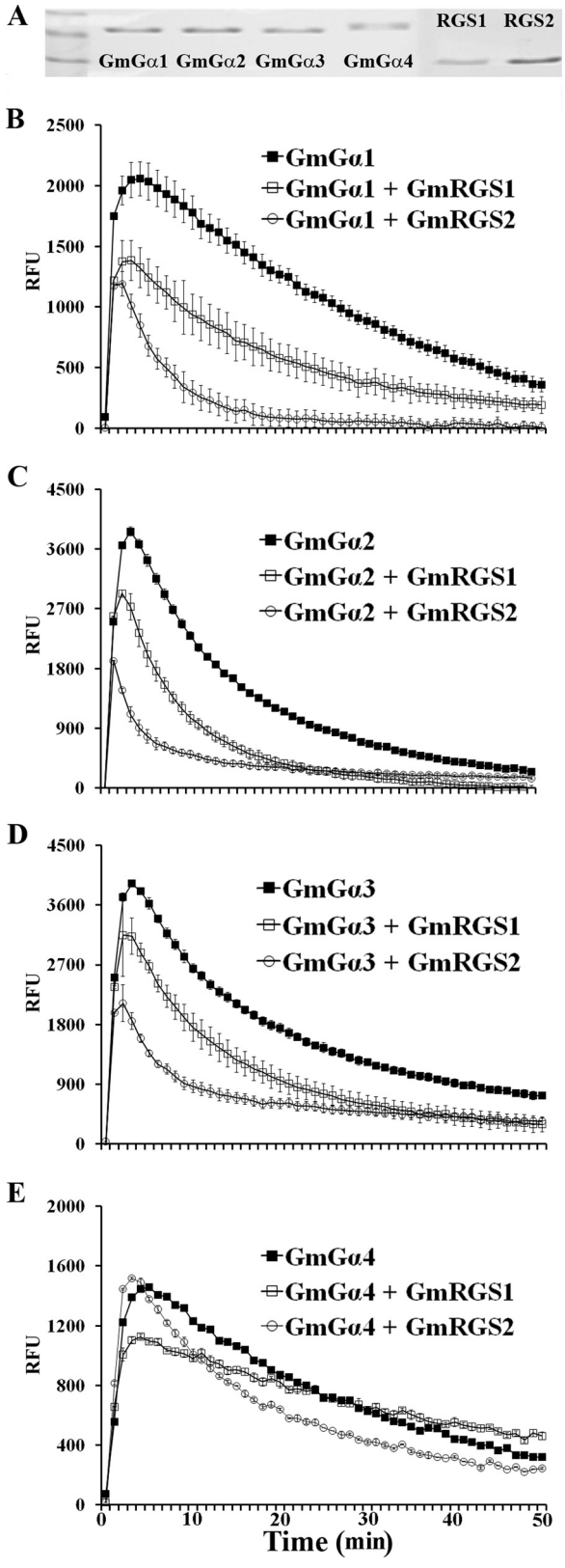

FIGURE 5. **GmRGS act as GAPs for GmGα.** *A,* SDS-PAGE analysis of purified recombinant GmGα1–4 and RGS domains (amino acids 251–464) of GmRGS1 and GmRGS2. *B–E,* effect of GmRGS1 and GmRGS2 on GTPase activity of GmGα1 (*B*), GmGα2 (*C*), GmGα3 (*D*), and GmGα4 (*E*). GTP hydrolysis was measured by using GTP-BODIPY-FL in real time fluorescence assays. Data are one of two independent experiments, each with three replicates, mean ± S.D.

denotes GTPase activity (Fig. 5, *B–E*). As reported previously, the group I GmGα were slower GTPases than the group II GmGα (23). Both GmRGS1 and GmRGS2 accelerated the GTPase activity of each GmGα, as evident by the steeper slopes for GTP hydrolysis (Fig. 5, *B–E*). Interestingly, the GTPase activity of all four GmGα was appreciably higher in the presence of GmRGS2 than GmRGS1 (Fig. 5, *B–E*), suggesting GmRGS2 as a more active GAP than GmRGS1.

BODIPY-based assays record the overall fluorescence emission resulting from simultaneous GTP binding and GTP hydrolysis and therefore at best provide initial information but not accurate estimation of the rates. To measure the distinct activities of the GmGα proteins and the steady-state GAP activity of the GmRGS, an assay that allowed for quantification of P_i release was used. These assays confirmed the results obtained in the BODIPY-based fluorescence assay that GmRGS2 was more active than GmRGS1 (Fig. 6 and Table 2). Furthermore, the rate of P_i released from the group II GmGα was faster than the group I GmGα in the presence of both GmRGS1 and GmRGS2 (Table 2). GmGα1 and GmGα3 have similar EC_{50} values for both GmRGS1 and GmRGS2, whereas GmGα2 and GmGα4 have ~3-fold higher EC_{50} for GmRGS1 than GmRGS2.

A glutamate at position 320 of AtRGS1 is crucial for GAP activity and its interaction with AtGPA1 (28). This residue is conserved in both GmRGS1 and GmRGS2 proteins (*Glu319*; Fig. 2*B*). To test the role of this residue in GmRGS, the E319K, E319Q, and E319A variants of GmRGS2 were generated. Using GmGα1 and GmGα2 as representatives of the group I and group II enzymes, the effect of GmRGS2 mutants on P_i release was examined (Fig. 7 and Table 3). This analysis showed that all three mutations decreased the GAP activity of GmRGS2 for both GmGα1 and GmGα2. In general, the V_{max} values decreased and EC_{50} values increased for each protein combination compared with wild-type GmRGS2 (Fig. 7 and Table 3). The E319A mutant displayed the largest effect and almost completely abolished the GAP activity of GmRGS2 (Table 3).

Amino Acid 357 Modulates GAP Activity in GmRGS—Sequence comparisons of GmRGS1 and GmRGS2 identified variations that may alter GAP activity. Of the six amino acid differences between the RGS domains of GmRGS1 and GmRGS2 (Fig. 2*B*), four are similar substitutions but two (positions 306 and 357) differ. Leu-306 in GmRGS1 is not conserved among different species; however, most plant and some animal RGS proteins, including AtRGS1 and GmRGS2, have a conserved alanine at position 357 (Fig. 2*B*). This residue is replaced with a valine in GmRGS1.

To test the potential role of this residue in controlling GAP activity, mutations in both GmRGS1 (V357A) and in GmRGS2 (A357V) were generated, and the mutant proteins were tested for their effect on GTPase activity of GmGα proteins. For these experiments, GmGα1 and GmGα2 were used as representatives of slower and faster GTPases, respectively. As shown in Fig. 8 and summarized in Table 4, mutation of residue 357 in each GmRGS switches GAP activity. The GmRGS1 V357A mutant enhances GTPase activity of GmGα compared with wild-type GmRGS1. Conversely, GmRGS2 A357V impairs the GTPase activity of GmGα compared with wild-type protein.

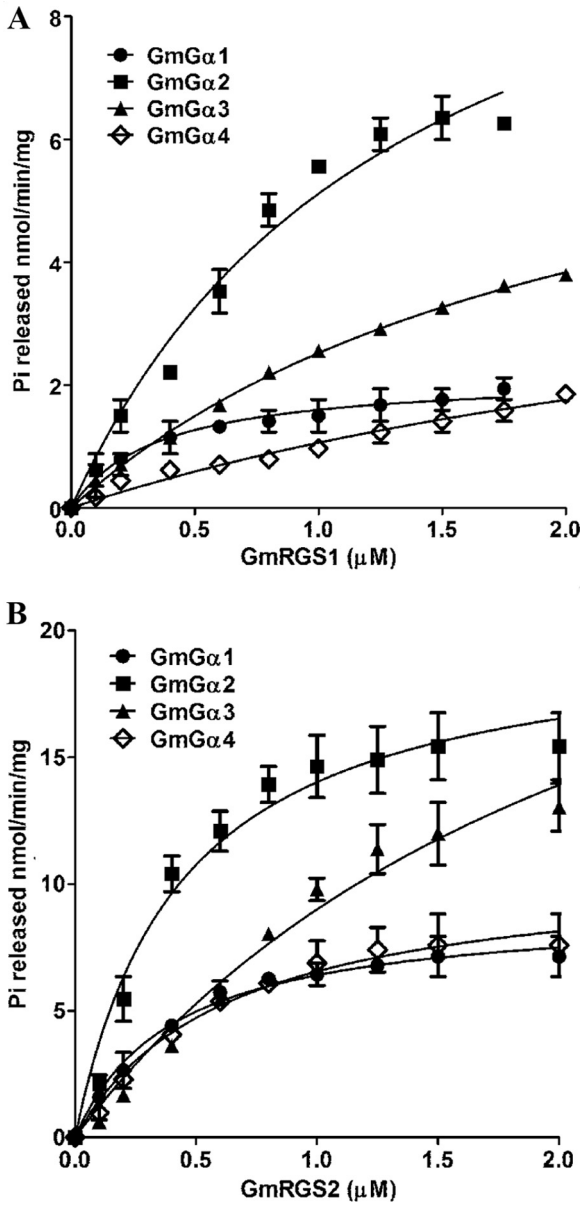

FIGURE 6. **GmRGS1 and GmRGS2 have distinct GAP activities on different GmGα.** *A,* rate of P_i release due to the GTPase activity of different GmGα in the presence of varying concentrations of GmRGS1. *B,* rate of P_i release from different GmGα in the presence of varying concentrations of GmRGS2. Experiments were repeated three times, and data were averaged. *Error bars* represent the mean ± S.E. Data were fit using GraphPad Prism version 5.0.

TABLE 2

Kinetics of phosphate (P_i) release from GmGα1–4 in the presence of GmRGS1 and GmRGS2

All values are expressed as a mean ± S.E. ($n = 3$).

Proteins	GmRGS1		GmRGS2	
	V_{max}	EC_{50}	V_{max}	EC_{50}
	nmol min^{-1} mg^{-1}	*μM*	*nmol min^{-1} mg^{-1}*	*μM*
GmGα1	2.1 ± 0.2	0.4 ± 0.1	9.5 ± 0.6	0.4 ± 0.1
GmGα2	11.6 ± 1.4	1.2 ± 0.3	21.7 ± 1.3	0.5 ± 0.1
GmGα3	7.2 ± 0.8	1.8 ± 0.3	27.7 ± 5.7	1.8 ± 0.7
GmGα4	3.4 ± 1. 7	2.3 ± 1.7	11.9 ± 1.1	0.7 ± 0.2

Additionally, GmRGS1 V357A reduces the EC_{50} difference seen in the wild-type GmRGS1 interactions with GmGα1 and GmGα2. GmRGS2 A357V has the opposite effect, leading to differences in the EC_{50}.

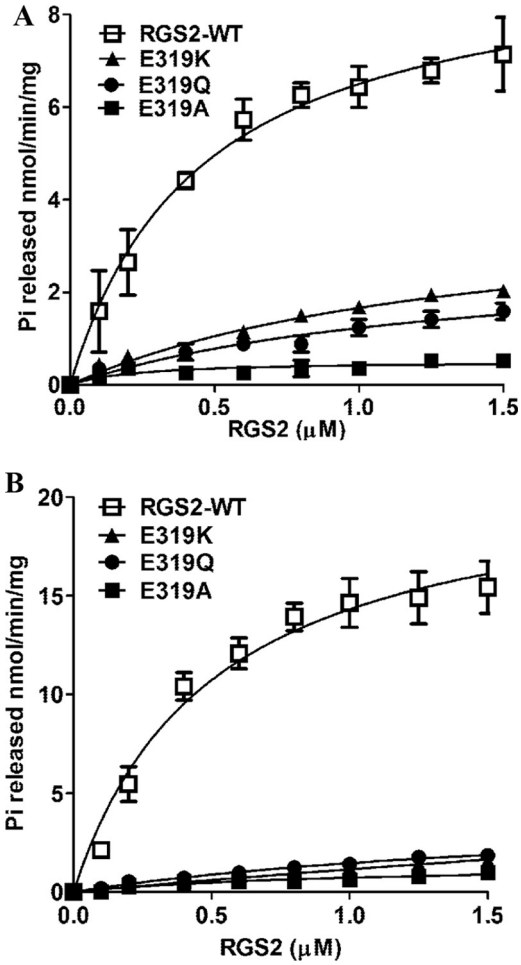

FIGURE 7. **Glu-319 is crucial for RGS protein activity.** *A,* rate of P_i release from GmGα1 in the presence of different concentrations of wild-type and mutant GmRGS2. *B,* rate of P_i release from GmGα2 in the presence of different concentrations of wild-type and mutant GmRGS2. Experiments were repeated three times, and data were averaged. *Error bars* represent the mean ± S.E. Data were fit using GraphPad Prism version 5.0.

TABLE 3

Effect of Glu-319 mutation in GmRGS2 on the rate of phosphate (P_i) release from GmGα1 and GmGα2

All values are expressed as a mean ± S.E. ($n = 3$).

Proteins	GmGα1		GmGα2	
	V_{max}	EC_{50}	V_{max}	EC_{50}
	nmol min^{-1} mg^{-1}	*μM*	*nmol min^{-1} mg^{-1}*	*μM*
RGS2-WT	9.5 ± 0.7	0.5 ± 0.1	21.5 ± 1.8	0.5 ± 0.1
RGS2-E319K	4.0 ± 0.6	1.4 ± 0.4	12.5 ± 0.4	10.0 ± 0.4
RGS2-E319Q	2.9 ± 0.7	1.3 ± 0.5	4.4 ± 0.5	2.0 ± 0.5
RGS2-E319A	0.5 ± 0.1	0.2 ± 0.1	1.5 ± 0.4	1.1 ± 0.4

DISCUSSION

Since the discovery of the *Arabidopsis* Gα protein AtGPA1 and its regulatory RGS protein AtRGS1 (11), almost all research related to the kinetics and regulation of plant G-protein signaling has remained focused on these two proteins. The presence of a single copy of each of these genes in the *Arabidopsis* genome and the availability of complete genetic knock-out mutants have allowed for the evaluation of the role of both these proteins on overall growth and development of *Arabidopsis*, a situation not feasible with most multicellular organisms (12). These studies have also provided important clues to alter-

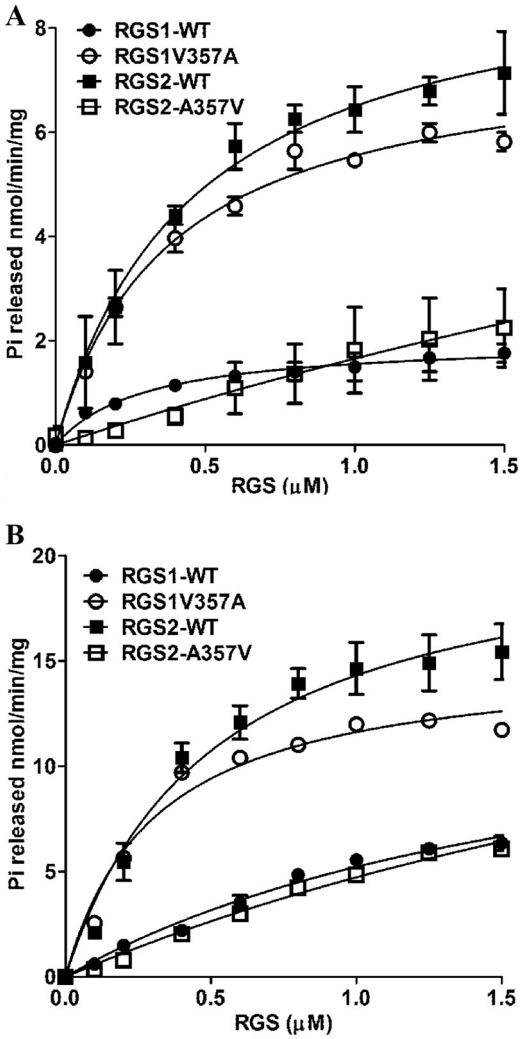

FIGURE 8. **Amino acid 357 determines differential GAP activities of GmRGS.** *A,* rate of P_i release from GmGα1 in the presence of different concentrations of wild-type and mutant GmRGS1 and GmRGS2. *B,* rate of P_i release from GmGα2 in the presence of wild-type and mutant GmRGS1 and GmRGS2. Experiments were repeated three times and data were averaged. *Error bars* represent the mean ± S.E. Data were fit using GraphPad Prism version 5.0.

TABLE 4

Effect of the V357A mutation in GmRGS1 and the A357V mutation in GmRGS2 on the rate of phosphate (P_i) release from GmGα1 and GmGα2

All values are expressed as a mean ± S.E. ($n = 3$).

Proteins	GmGα1		GmGα2	
	V_{max}	EC_{50}	V_{max}	EC_{50}
	nmol min^{-1} mg^{-1}	μM	*nmol min^{-1} mg^{-1}*	μM
RGS1-WT	2.0 ± 0.2	0.4 ± 0.1	15.0 ± 2.4	1.9 ± 0.5
RGS1-V357A	7.6 ± 0.3	0.3 ± 0.1	15.2 ± 0.8	0.3 ± 0.0
RGS2-WT	9.5 ± 0.8	0.5 ± 0.1	21.5 ± 0.2	0.5 ± 0.1
RGS2-A357V	13.4 ± 0.2	7.1 ± 0.2	22.8 ± 1.5	3.8 ± 1.2

native G-protein signaling mechanisms beyond the canonical mammalian models. However, the simple G-protein system of *Arabidopsis* limits our view of the variability and complexity of plant G-protein networks and does not allow for a comparative assessment of their biochemical properties. The presence of multiple copies of all the G-protein signaling proteins in soybean provides an opportunity to extend the knowledge to more complex and agriculturally relevant plants, as more than 70% of plants are polyploid and likely have multiple copies of G-proteins, unlike *Arabidopsis* or rice.

Biochemical Properties of Gα and RGS Proteins of Soybean—Biochemical characterization of the four soybean Gα proteins reveals rates of GTP binding 100–1000-fold faster than mammalian systems, along with higher rates of GDP release and lower rates of GTP hydrolysis (Fig. 1). On the whole, these data are similar to AtGPA1, which has an observed rate of GTP binding 2 orders of magnitude faster and a steady-state rate of GTP hydrolysis an order of magnitude slower than the mammalian Gαo (28), implying that GTP hydrolysis is likely to be the rate-limiting step in plant G-protein signaling. Nevertheless, important differences were observed in the kinetics of the four GmGα proteins (Fig. 1 and Table 1). GmGα4 has a rate of GTP binding 4-fold higher than GmGα2 and GmGα3, whereas the rate of GDP dissociation from GmGα3 is nearly 5-fold slower than that of GmGα1 and GmGα4. These differences suggest variations in the timing of the G-protein cycle in soybean.

The rate-limiting step of the G-protein cycle in *Arabidopsis* is regulated by AtRGS1, which causes a 35-fold increase in the steady-state rate of GTP hydrolysis by AtGPA1 (31). Similar to AtRGS1, both GmRGS1 and GmRGS2 act as GAPs. Direct biochemical analyses confirmed a significant increase in the rate of GTP hydrolysis for each of the GmGα proteins in the presence of GmRGS proteins (Figs. 5 and 6). Interestingly, despite 96% sequence identity between the two GmRGS proteins, the GAP activity of GmRGS2 is up to 5-fold greater than that of GmRGS1, depending on the Gα protein assayed (Fig. 6). This suggests that the G-protein cycle mediated by each of the four GmGα could have different kinetics subject to its regulation by either GmRGS1 or GmRGS2, in addition to RGS-independent regulation.

How these moderately different biochemical properties and their regulation affect G-protein cycling in a cell with respect to sharing the available pool of GTP and respond to a particular signal remains an open question at this juncture. Moreover, because the interaction of Gα proteins with G$\beta\gamma$ dimers and/or other effector proteins of G-protein signaling complex depends on GDP-bound *versus* GTP-bound conformation of Gα proteins (44), it is conceivable that the inherent biochemical differences and their distinct regulation will also affect the downstream signaling pathways initiated by each Gα protein. These differences provide a first glimpse of the possible complexity of G-protein cycle in plants, especially if more than one protein is active in any given cell type.

In some cases, a high degree of tissue- or developmental stage-dependent expression of specific genes as well as a high degree of overlap between specific *GmRGS* and *GmGα* gene expression exists. For example, during seed development, the expression of *GmRGS1* follows a similar trend as the group II *GmGα*, whereas the expression of *GmRGS2* overlaps with the group I *GmGα* (Fig. 3*C*) (23). Conversely, during seed germination, an opposite trend occurs as both *GmRGS* genes are down-regulated following imbibition (Fig. 3*D*), but the *GmGα* genes are up-regulated (23). It is possible that different modes of G-protein signaling are active during specific physiological

responses. An RGS-independent signaling pathway may operate during seed germination *versus* an active RGS-dependent signaling pathway during seed development. Further studies focused toward identifying the signal-dependent *in vivo* changes in individual G-protein activation and cycling, elucidation of signal-dependent protein complexes, and in depth cell-specific and signal-dependent expression profiling of individual GmGα will help answer some of these questions.

Interaction between GmGα and GmRGS Proteins—According to the mammalian paradigm, the GAP activity of RGS proteins depends on their physical interaction with cognate Gα proteins (3, 4, 7). Both GmRGS proteins interacted with all four GmGα in the yeast-split ubiquitin assays and bimolecular fluorescence complementation assays *in planta* (Fig. 4). We did not observe any significant difference in interaction strengths between specific Gα and RGS protein pairs in these assays, despite noticeable differences in the GAP activity of each GmRGS protein. However, it is interesting to note that the EC_{50} values, which approximate the equilibrium-binding constants, indicate preferences of each GmRGS for certain GmGα. To fully understand this, more quantitative methods such as isothermal titration calorimetry will need to be used to directly measure the strength of these interactions.

In AtRGS1, a glutamate in a putative α-helical region is important for both GAP activity and interaction with AtGPA1 based on homology modeling using the human RGS4-Giα1 interaction (45). This residue is conserved in the GmRGS, and our mutant analysis showed that changing either its polarity and/or charge has a significant effect on the GAP activity of both proteins (Fig. 7 and Table 3). Although these data suggested that the overall interaction interface of plant and mammalian RGS-Gα interaction may be conserved, the presence of two different RGS proteins also offered an opportunity to identify key amino acids responsible for their differential GAP activities. Interestingly, the amino acid at position 357 (*i.e.* valine or alanine), identified in this study as a molecular switch that controls the slow *versus* fast GAP activities of GmRGS1 and GmRGS2 (Fig. 8 and Table 4), was not previously predicted to be directly involved in RGS-Gα interaction (45). It would therefore be premature to draw conclusions about the plant Gα-RGS interaction interface at this point. Structural information on the interaction of a plant Gα and its cognate RGS protein would help define the protein-protein interface in the plant system, especially in light of the recent crystal structure of AtGPA1 that has shown unique, plant-specific features (29).

RGS Proteins in the Context of Plant Evolution—Based on two genome duplication events during soybean evolution (38), four RGS proteins were expected; however, our analysis identified only two GmRGS (Fig. 2). This suggests a likely loss of the other two genes during evolution. Most dicot plants have one or more homologs of RGS proteins, although *Setaria* is the sole representative monocot with an RGS protein homolog. The absence of a 7TM domain in the RGS protein from *Setaria* suggests the possibility that the 7TM domain was lost first during evolution, followed by a subsequent loss of RGS proteins in the monocot lineage.

The absence of an RGS protein homolog from almost the entire monocot plant lineage warrants a detailed evolutionary analysis of the regulation of G-protein cycle in monocot *versus* dicot plants (supplemental Fig. S1). It has been shown for *Arabidopsis* and in this report that RGS protein-regulated acceleration of GTPase activity is a crucial step in the plant G-protein cycle. If the role of the RGS proteins is only to accelerate the extremely slow GTPase activity of the dicot Gα proteins so that they continue cycling between the GDP-bound and GTP-bound forms, then the Gα proteins in monocots might have different kinetic properties and may not require the GTPase acceleration by an RGS protein. Interestingly, there is one report indicating that the rates of GTP binding and GDP release of the rice Gα protein RGA1 are comparable with those of the mammalian Gα proteins and significantly different from AtGPA1 (46); however, these data remain contested (31, 47). In this context, it is also interesting to note that the overall phenotypes of the *Atgpa1* mutants are significantly different from the *Osrga1* mutants (8, 12). The extent to which the presence of an RGS protein in the plant genome correlates with the presence of a slow *versus* fast GTPase will only become clear after detailed biochemical characterization of the Gα proteins from evolutionarily different plant lineages. Furthermore, the presence of a 7TM GPCR-like domain in plant RGS proteins is intriguing. Data available from AtRGS1 suggests that this domain does not have a guanine nucleotide exchange factor activity on AtGPA1, at least with sugar as a ligand (28, 31). Whether other compounds may act as a ligand for the 7TM domain of plant RGS proteins remains to be seen. Because this domain does not interact with the Gα protein, it may act as a targeting or scaffolding protein. It could also act in pathways not related to G-protein signaling similar to many mammalian RGS domain-containing proteins (48). Continued sequence analysis of additional plant genomes at important evolutionary junctions will help solve this enigma and shed light on the evolution of plant-specific G-protein signaling pathways.

Biological Significance of Different Kinetic Properties of GmGα and GmRGS Proteins—Studies outside of the rigorously studied mammalian models are beginning to reveal that the basic biochemistry of Gα proteins, *i.e.* specific binding of guanine nucleotides, inherent GTPase activity with bound GTP, and regulation by RGS proteins, is conserved across phyla. Similarly, the core interactions between different components of the G-protein complex are also fully conserved in each of the organisms studied to date, *e.g.* the interaction between Gα-GDP and G$\beta\gamma$, the nondissociable interaction of Gβ and Gγ, and the interaction of Gα and RGS domains.

Nonetheless, it is becoming increasingly clear that the same basic set of biochemical reactions and core protein interactions have evolved to act via significantly different mechanisms that fine-tune individual steps in this timing cycle. Studies in *Arabidopsis* revealed a perplexing picture of plant G-protein signaling, as a limited number of G-protein complex components seem to regulate a multitude of signaling pathways, although plants lacking one or more of these proteins display relatively subtle phenotypes (12). It has been suggested that G-protein signaling in plants evolved to suit their stationary life style by regulating overall growth and development under any given environmental condition rather than exerting absolute control of any particular pathway (17, 49). The presence of multiple

proteins with moderately different kinetics and regulation in soybean (and in other polyploid plant species) presents a scenario in which such principles can be applied even more effectively. It can be envisioned that not only the multiplicity of the components and their specific expression patterns but also their biochemical properties will contribute to generate networks of functionally dissimilar protein complexes to effectively tune the response of a plant to a variety of signals. It is possible that these modest kinetic differences observed *in vitro* may result in significantly greater changes *in vivo* in terms of signal output depending on the interaction network of specific G-protein complexes. Future research focused toward elucidating the signal-dependent G-protein complexes, their regulation of specific physiological responses, and modeling of different interactions in the context of their effect on amplifying or dampening the signal output will significantly improve our understanding of G-protein signaling pathways in plants.

Acknowledgments—We thank Dr. Jan A. Miernyk (University of Missouri, Columbia) for providing different developmental stages of soybean seeds; Dr. Petra Levin (Washington University, St. Louis) for allowing the use of the Olis DM45 spectrofluorimeter; Christine E. Barnickol for editing of the manuscript, and two anonymous reviewers for their excellent suggestions for improving the manuscript.

REFERENCES

1. Offermanns, S. (2003) G-proteins as transducers in transmembrane signaling. *Prog. Biophys. Mol. Biol.* **83,** 101–130
2. Cabrera-Vera, T. M., Vanhauwe, J., Thomas, T. O., Medkova, M., Preininger, A., Mazzoni, M. R., and Hamm, H. E. (2003) Insights into G protein structure, function, and regulation. *Endocr. Rev.* **24,** 765–781
3. Wettschureck, N., and Offermanns, S. (2005) Mammalian G proteins and their cell type-specific functions. *Physiol. Rev.* **85,** 1159–1204
4. Siderovski, D. P., and Willard, F. S. (2005) The GAPs, GEFs, and GDIs of heterotrimeric G-protein α subunits. *Int. J. Biol. Sci.* **1,** 51–66
5. Johnston, C. A., and Siderovski, D. P. (2007) Receptor-mediated activation of heterotrimeric G-proteins. Current structural insights. *Mol. Pharmacol.* **72,** 219–230
6. Oldham, W. M., and Hamm, H. E. (2008) Heterotrimeric G protein activation by G-protein-coupled receptors. *Nat. Rev. Mol. Cell Biol.* **9,** 60–71
7. Lambert, N. A., Johnston, C. A., Cappell, S. D., Kuravi, S., Kimple, A. J., Willard, F. S., and Siderovski, D. P. (2010) Regulators of G-protein signaling accelerate GPCR signaling kinetics and govern sensitivity solely by accelerating GTPase activity. *Proc. Natl. Acad. Sci. U.S.A.* **107,** 7066–7071
8. Temple, B. R., and Jones, A. M. (2007) The plant heterotrimeric G-protein complex. *Annu. Rev. Plant. Biol.* **58,** 249–266
9. Jones, A. M., and Assmann, S. M. (2004) Plants. The latest model system for G-protein research. *EMBO. Rep.* **5,** 572–578
10. Pandey, S. (2011) More (G-proteins) please! Identification of an elaborate network of G-proteins in soybean. *Plant. Signal. Behav.* **6,** 780–782
11. Chen, J. G., Willard, F. S., Huang, J., Liang, J., Chasse, S. A., Jones, A. M., and Siderovski, D. P. (2003) A seven-transmembrane RGS protein that modulates plant cell proliferation. *Science* **301,** 1728–1731
12. Perfus-Barbeoch, L., Jones, A. M., and Assmann, S. M. (2004) Plant heterotrimeric G protein function. Insights from *Arabidopsis* and rice mutants. *Curr. Opin. Plant Biol.* **7,** 719–731
13. Wang, X. Q., Ullah, H., Jones, A. M., and Assmann, S. M. (2001) G protein regulation of ion channels and abscisic acid signaling in *Arabidopsis* guard cells. *Science* **292,** 2070–2072
14. Ullah, H., Chen, J. G., Young, J. C., Im, K. H., Sussman, M. R., and Jones, A. M. (2001) Modulation of cell proliferation by heterotrimeric G protein in *Arabidopsis*. *Science* **292,** 2066–2069
15. Ullah, H., Chen, J. G., Temple, B., Boyes, D. C., Alonso, J. M., Davis, K. R., Ecker, J. R., and Jones, A. M. (2003) The β-subunit of the *Arabidopsis* G protein negatively regulates auxin-induced cell division and affects multiple developmental processes. *Plant Cell* **15,** 393–409
16. Trusov, Y., Rookes, J. E., Tilbrook, K., Chakravorty, D., Mason, M. G., Anderson, D., Chen, J. G., Jones, A. M., and Botella, J. R. (2007) Heterotrimeric G protein γ subunits provide functional selectivity in G$\beta\gamma$ dimer signaling in *Arabidopsis*. *Plant Cell* **19,** 1235–1250
17. Nilson, S. E., and Assmann, S. M. (2010) Heterotrimeric G proteins regulate reproductive trait plasticity in response to water availability. *New Phytol.* **185,** 734–746
18. Warpeha, K. M., Gibbons, J., Carol, A., Slusser, J., Tree, R., Durham, W., and Kaufman, L. S. (2008) Adequate phenylalanine synthesis mediated by G protein is critical for protection from UV radiation damage in young etiolated *Arabidopsis thaliana* seedlings. *Plant Cell Environ.* **31,** 1756–1770
19. Pandey, S., Monshausen, G. B., Ding, L., and Assmann, S. M. (2008) Regulation of root-wave response by extra large and conventional G proteins in *Arabidopsis thaliana*. *Plant J.* **55,** 311–322
20. Suharsono, U., Fujisawa, Y., Kawasaki, T., Iwasaki, Y., Satoh, H., and Shimamoto, K. (2002) The heterotrimeric G protein α subunit acts upstream of the small GTPase Rac in disease resistance of rice. *Proc. Natl. Acad. Sci. U.S.A.* **99,** 13307–13312
21. Ueguchi-Tanaka, M., Fujisawa, Y., Kobayashi, M., Ashikari, M., Iwasaki, Y., Kitano, H., and Matsuoka, M. (2000) Rice dwarf mutant d1, which is defective in the α subunit of the heterotrimeric G protein, affects gibberellin signal transduction. *Proc. Natl. Acad. Sci. U.S.A.* **97,** 11638–11643
22. Choudhury, S. R., Bisht, N. C., Thompson, R., Todorov, O., and Pandey, S. (2011) Conventional and novel Gγ protein families constitute the heterotrimeric G-protein signaling network in soybean. *PLoS One* **6,** e23361
23. Bisht, N. C., Jez, J. M., and Pandey, S. (2011) An elaborate heterotrimeric G-protein family from soybean expands the diversity of plant G-protein networks. *New Phytol.* **190,** 35–48
24. Pronin, A. N., and Gautam, N. (1992) Interaction between G-protein β and γ subunit types is selective. *Proc. Natl. Acad. Sci. U.S.A.* **89,** 6220–6224
25. Li, Y., Sternweis, P. M., Charnecki, S., Smith, T. F., Gilman, A. G., Neer, E. J., and Kozasa, T. (1998) Sites for Gα binding on the G protein β subunit overlap with sites for regulation of phospholipase Cβ and adenylyl cyclase. *J. Biol. Chem.* **273,** 16265–16272
26. Thomas, T. C., Schmidt, C. J., and Neer, E. J. (1993) G-protein α o subunit. mutation of conserved cysteines identifies a subunit contact surface and alters GDP affinity. *Proc. Natl. Acad. Sci. U.S.A.* **90,** 10295–10299
27. Schmidt, C. J., Thomas, T. C., Levine, M. A., and Neer, E. J. (1992) Specificity of G protein β and γ subunit interactions. *J. Biol. Chem.* **267,** 13807–13810
28. Johnston, C. A., Taylor, J. P., Gao, Y., Kimple, A. J., Grigston, J. C., Chen, J. G., Siderovski, D. P., Jones, A. M., and Willard, F. S. (2007) GTPase acceleration as the rate-limiting step in *Arabidopsis* G protein-coupled sugar signaling. *Proc. Natl. Acad. Sci. U.S.A.* **104,** 17317–17322
29. Jones, J. C., Duffy, J. W., Machius, M., Temple, B. R., Dohlman, H. G., and Jones, A. M. (2011) The crystal structure of a self-activating G protein α subunit reveals its distinct mechanism of signal initiation. *Sci. Signal.* **4,** ra8
30. Jones, J. C., Temple, B. R., Jones, A. M., and Dohlman, H. G. (2011) Functional reconstitution of an atypical G protein heterotrimer and regulator of G protein signaling protein (RGS1) from *Arabidopsis thaliana*. *J. Biol. Chem.* **286,** 13143–13150
31. Johnston, C. A., Willard, M. D., Kimple, A. J., Siderovski, D. P., and Willard, F. S. (2008) A sweet cycle for *Arabidopsis* G-protein. Recent discoveries and controversies in plant G-protein signal transduction. *Plant Signal. Behav.* **3,** 1067–1076
32. Jez, J. M., and Cahoon, R. E. (2004) Kinetic mechanism of glutathione synthetase from *Arabidopsis thaliana*. *J. Biol. Chem.* **279,** 42726–42731
33. Pandey, S., and Assmann, S. M. (2004) The *Arabidopsis* putative G protein-coupled receptor GCR1 interacts with the G protein α subunit GPA1 and regulates abscisic acid signaling. *Plant Cell* **16,** 1616–1632
34. Citovsky, V., Lee, L. Y., Vyas, S., Glick, E., Chen, M. H., Vainstein, A., Gafni, Y., Gelvin, S. B., and Tzfira, T. (2006) Subcellular localization of

interacting proteins by bimolecular fluorescence complementation *in planta*. *J. Mol. Biol.* **362,** 1120–1131
35. Johnson, K. A. (2009) Fitting enzyme kinetic data with KinTek Global Kinetic Explorer. *Methods Enzymol.* **467,** 601–626
36. Pandey, S., Nelson, D. C., and Assmann, S. M. (2009) Two novel GPCR-type G proteins are abscisic acid receptors in *Arabidopsis*. *Cell* **136,** 136–148
37. Anantharaman, V., Abhiman, S., de Souza, R. F., and Aravind, L. (2011) Comparative genomics uncovers novel structural and functional features of the heterotrimeric GTPase signaling system. *Gene* **475,** 63–78
38. Schmutz, J., Cannon, S. B., Schlueter, J., Ma, J., Mitros, T., Nelson, W., Hyten, D. L., Song, Q., Thelen, J. J., and Cheng, J., Xu, D., Hellsten, U., May, G. D., Yu, Y., Sakurai, T., Umezawa, T., Bhattacharyya, M. K., Sandhu, D., Valliyodan, B., Lindquist, E., Peto, M., Grant, D., Shu, S., Goodstein, D., Barry, K., Futrell-Griggs, M., Abernathy, B., Du, J., Tian, Z., Zhu, L., Gill, N., Joshi, T., Libault, M., Sethuraman, A., Zhang, X. C., Shinozaki, K., Nguyen, H. T., Wing, R. A., Cregan, P., Specht, J., Grimwood, J., Rokhsar, D., Stacey, G., Shoemaker, R. C., and Jackson, S. A. (2010) Genome sequence of the palaeopolyploid soybean. *Nature* **463,** 178–183
39. Roy, A., Kucukural, A., and Zhang, Y. (2010) I-TASSER. A unified platform for automated protein structure and function prediction. *Nat. Protoc.* **5,** 725–738
40. Sun, J., Miwa, H., Downie, J. A., and Oldroyd, G. E. (2007) Mastoparan activates calcium spiking analogous to Nod factor-induced responses in *Medicago truncatula* root hair cells. *Plant Physiol.* **144,** 695–702
41. Hajduch, M., Hearne, L. B., Miernyk, J. A., Casteel, J. E., Joshi, T., Agrawal, G. K., Song, Z., Zhou, M., Xu, D., and Thelen, J. J. (2010) Systems analysis of seed filling in *Arabidopsis*. Using general linear modeling to assess concordance of transcript and protein expression. *Plant Physiol.* **152,** 2078–2087
42. Soundararajan, M., Willard, F. S., Kimple, A. J., Turnbull, A. P., Ball, L. J., Schoch, G. A., Gileadi, C., Fedorov, O. Y., Dowler, E. F., Higman, V. A., Hutsell, S. Q., Sundström, M., Doyle, D. A., and Siderovski, D. P. (2008) Structural diversity in the RGS domain and its interaction with heterotrimeric G protein α-subunits. *Proc. Natl. Acad. Sci. U.S.A.* **105,** 6457–6462
43. Kosloff, M., Travis, A. M., Bosch, D. E., Siderovski, D. P., and Arshavsky, V. Y. (2011) Integrating energy calculations with functional assays to decipher the specificity of G protein-RGS protein interactions. *Nat. Struct. Mol. Biol.* **18,** 846–853
44. Klopffleisch, K., Phan, N., Augustin, K., Bayne, R. S., Booker, K. S., Botella, J. R., Carpita, N. C., Carr, T., Chen, J. G., Cooke, T. R., Frick-Cheng, A., Friedman, E. J., Fulk, B., Hahn, M. G., Jiang, K., Jorda, L., Kruppe, L., Liu, C., Lorek, J., McCann, M. C., Molina, A., Moriyama, E. N., Mukhtar, M. S., Mudgil, Y., Pattathil, S., Schwarz, J., Seta, S., Tan, M., Temp, U., Trusov, Y., Urano, D., Welter, B., Yang, J., Panstruga, R., Uhrig, J. F., and Jones, A. M. (2011) *Arabidopsis* G-protein interactome reveals connections to cell wall carbohydrates and morphogenesis. *Mol. Syst. Biol.* **7,** 532
45. Tesmer, J. J., Berman, D. M., Gilman, A. G., and Sprang, S. R. (1997) Structure of RGS4 bound to AlF^{4-}-activated $G_i\alpha_1$. Stabilization of the transition state for GTP hydrolysis. *Cell* **89,** 251–261
46. Seo, H. S., Jeong, J. Y., Nahm, M. Y., Kim, S. W., Lee, S. Y., and Bahk, J. D. (2003) The effect of pH and various cations on the GTP hydrolysis of rice heterotrimeric G-protein α subunit expressed in *Escherichia coli*. *J. Biochem. Mol. Biol.* **36,** 196–200
47. Iwasaki, Y., Kato, T., Kaidoh, T., Ishikawa, A., and Asahi, T. (1997) Characterization of the putative α subunit of a heterotrimeric G protein in rice. *Plant Mol. Biol.* **34,** 563–572
48. Bansal, G., Druey, K. M., and Xie, Z. (2007) R4 RGS proteins: regulation of G-protein signaling and beyond. *Pharmacol. Ther.* **116,** 473–495
49. Assmann, S. M. (2004) Plant G proteins, phytohormones, and plasticity. Three questions and a speculation. *Sci. STKE 2004,* re20